

## SYSTEM STABILITY DESIGN CRITERIA FOR ALUMINUM STRUCTURES

Ronald D. Ziemian\* and J. Randolph Kissell \*\*

\* Bucknell University, Lewisburg, PA, USA  
e-mail: ziemian@bucknell.edu

\*\* The TGB Partnership, Hillsborough, NC, USA  
e-mail: randy.kissell@tgbpartnership.com

**Keywords:** Aluminum structures; Second-order effects, Stability, Direct analysis.

**Abstract.** *The 2010 Aluminum Association Specification for Aluminum Structures has been significantly revised to include more transparent stability provisions. Second-order effects, including  $P-\Delta$  and  $P-\delta$  moments, and factors known to accentuate these effects, such as geometric imperfections and member inelasticity, will need to be considered in determining required strengths. This paper provides an overview of these provisions and describes experimental and analytical studies that investigated their effectiveness.*

### 1 INTRODUCTION

Widely used in the US since its first publication in 1967, the Aluminum Association's (AA) *Specification for Aluminum Structures* [1] has always addressed the stability of individual structural members. With regard to beams and columns, the Specification provides equations for determining the strength of beams and columns that account for local buckling of elements such as flanges or webs, and flexural, flexural-torsional, and lateral-torsional buckling of members. Prior to the 2010 Specification, a moment-amplification factor was used to address the  $P-\delta$  effect, which is the effect of axial load acting on the deflected shape of a member between its ends, on the stability of beam-columns.

Although it addressed the stability of individual members, earlier editions of the Specification have not directly considered the stability of structural systems as a whole. The Specification has never required engineers to design for the  $P-\Delta$  effect, which is the effect of loads acting on the displaced location of joints in a structure, and only in more recent editions of the Specification was system response included through the use of the effective length concept. As a result, the strength of a structural system designed by previous editions of the Specification can be significantly less than the strength of its weakest member.

With some collapses of aluminum structures attributed to system instability, the AA decided to provide more comprehensive and transparent stability provisions in the 2010 edition of the Specification. Recognizing that accurately determining the effective length of members is complicated by the wide variety of non-orthogonal structural geometries used in aluminum structures, the AA has abandoned the use of effective length. In an effort to be more consistent with other US design specifications, the AA adopted stability provisions similar to those that appear in the 2010 American Institute of Steel Construction's (AISC) *Specification for Structural Steel Buildings* [2]. Because of differences in (1) the stiffness and strength of steel and aluminum, in particular that the  $E/\sigma_y$  ratio for steel is approximately twice that of aluminum, and (2) the manufacturing processes of aluminum profiles and hot-rolled steel sections, a study that includes experimental and analytical components was conducted to confirm the adequacy of adopting the AISC provisions. A summary of this study is presented below.

## 2 STABILITY PROVISIONS - 2010 AA SPECIFICATION

In *Chapter C: Design for Stability*, the AA Specification provides analysis requirements (calculation of required strengths) and design requirements (calculation of available strengths) for the entire structural system and for each of its components. With respect to the latter, available strengths shall be based on the actual unbraced length of the member (i.e., an effective length factor of  $k = 1$ ). Required strengths are to be determined from an analysis that considers:

1. All member and connection deformation;
2. Second-order effects, including both  $P$ - $\Delta$  and  $P$ - $\delta$  moments;
3. Geometric imperfections, such as frame out-of-plumbness and member out-of-straightness, that reflect the tolerances permitted in contract documents;
4. Reductions in member stiffness due to:
  - a. inelasticity or partial yielding of members
  - b. uncertainty in defining the stiffness and strength of components.

As a means for reducing member stiffness due to inelasticity, the AA Specification requires that the flexural stiffness of all members be reduced by  $\tau$ , where

$$\begin{aligned} \tau &= 1.0 && \text{for } \frac{P}{P_y} \leq 0.5 \\ \tau &= 4 \left( \frac{P}{P_y} \right) \left( 1 - \frac{P}{P_y} \right) && \text{for } 0.5 < \frac{P}{P_y} \leq 1.0 \end{aligned} \quad (1)$$

in which  $P$ , is the required axial compressive strength (i.e., axial force in member) and  $P_y$  is the axial yield or squash load (i.e.,  $P_y = A_g \sigma_y$ ).

Because of uncertainty in the stiffness and strength of the structural system, there exists the potential for larger deflections (due to less than expected lateral stiffness) and correspondingly increased second-order moments. To account for this, a factor of 0.8 must be applied to all axial, flexural, and shear stiffnesses in the structure. One simple method for achieving this is to employ 80% of the actual modulus of elasticity in the analysis model.

In addition to the above analysis requirements, the Specification requires that all gravity loads must be included in the analysis of lateral load-resisting systems. For example, additional lateral load may result from columns that support only gravity loads but attain their sidesway stability by leaning on the structure's lateral system.

## 3 BASIS FOR STUDY

In general, the above analysis requirements should apply to any metal structure in which there is significance in formulating the equations of equilibrium on the deformed, and perhaps partially yielded, geometry of the structural system. Because the details in accounting for member inelasticity ( $\tau$ -factor of equation 1) and uncertainty in stiffness (stiffness reduction factor of 0.8) were specifically developed for steel buildings, their applicability to aluminum structures deserves to be investigated.

A good starting point is to provide a background to the AISC approach. The AISC Specification has long recognized the impact of residual stresses on the performance of hot rolled sections. Compressive axial stresses on the order of 30 to 50 percent of the material yield strength can result from the steel fabrication process and such stresses can obviously accentuate the partial yielding of a cross section as a member reaches a strength limit state (e.g., inelastic flexural buckling of a column). Based on an extensive calibration study [3], the AISC determined that the relatively simple parabolic expression provided by equation 1, which was originally developed by Bleich [4], and the stiffness reduction factor 0.8 adequately account for the loss in bending stiffness of members subject to high axial compressive loads. For frames with slender members, where the limit state is governed by elastic stability (i.e.,  $\tau = 1.0$

with  $P/P_y < 0.5$ ), the same 0.8 factor can be employed because it is approximately equal to the product of the AISC resistance factor of 0.9 and the 0.877 reduction factor used in the AISC column curve to account for member out-of-straightness.

In contrast, many aluminum sections are typically extruded and upon cooling are then pulled to straighten or remove any initial out-of-straightness. This stretching process requires axially straining the material beyond yield and as a result typically relieves the residual stresses that may have developed from an uneven cooling process. On the other hand, some aluminum sections are fabricated by welding several profiles together; a fabrication process that may result in significant residual stresses.

Differences in the stress-strain relationships for each material may also be a factor in determining the appropriateness of adopting the AISC provisions. Hot-rolled steels typically have a fairly linear constitutive relationship with a pronounced yield point. In contrast, the stress-strain relationships for most aluminum alloys are inherently nonlinear and without pronounced yield points [5]; as a result, “yield” for most aluminum alloys is defined by the stress at a 0.2% strain offset. Hence, the above reasons (e.g., absence of residual stresses) for not employing the parabolic form of equation 1 may be offset by the need to model a nonlinear material.

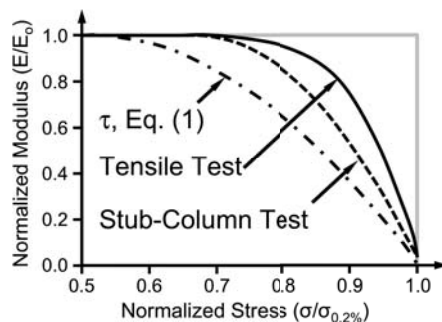
#### 4 EXPERIMENTAL STUDY

As an initial study, a series of stub-column tests were performed according to the Structural Stability Research Council’s *Technical Memorandum No. 3: Stub-Column Test Procedure* [6]. Using the experimental setup shown in figure 1(a), three I-shape sections and three hollow-rectangular shapes were compression tested. The dimensions for the I-shape are shown in figure 2 and the rectangular shape was  $203.2 \times 101.6$  mm with a wall thickness of 12.7 mm. In all tests, the stub-columns were 6061-T6 aluminum of length 0.61 m. In each test, the compression force and longitudinal deformation at two locations (mid-flange) over a gauge length of 254 mm were recorded. The force was converted to an axial stress and the deformations were averaged and then converted to axial strain. Stress-strain plots were then prepared for each of the specimens for the two shapes. For each shape, the stress-strain data was averaged to produce a single curve.

An untested fourth specimen for each shape was sectioned and tensile coupons were machined from material at two locations, including the flange tip and the flange-web intersection. Tensile tests were performed on these coupons according to ASTM B557 [7]. The two resulting stress-strain curves for the tension tests of each shape were averaged using the same procedure as that employed in the above compression tests.



(a)



(b)

Figure 1: Experimental setup and results of stub-column axial compressive tests.

For each shape, the resulting tensile and compressive stress-strain curves were used to determine a stiffness reduction relationship equivalent to that provided in equation 1. This was done by first determining the stress  $\sigma_{0.2\%}$  corresponding to a 0.2% offset strain and the modulus of elasticity  $E_0$  at low stress values (taken as the slope of line “best-fit” to stress-strain curve between  $0.15\sigma_{0.2\%}$  and  $0.65\sigma_{0.2\%}$ ). The stress  $\sigma$  normalized by  $\sigma_{0.2\%}$  and the corresponding tangent modulus  $E$  (slope of stress-strain curve) normalized by  $E_0$  are then plotted as shown in figure 1(b). Although this figure only includes the resulting tension and stub-column curves for the I-shape, similar results were obtained for the hollow-rectangular section.

A review of the three curves plotted in figure 1(b) indicate:

1. The stiffness relationship for tension confirms that the material has a significantly nonlinear response. A material with a linear stress-strain relationship and a pronounced yield point would closely match the grey bi-linear curve shown in the upper right of the figure.
2. In comparison to the tension response, the compression relationship indicates that the material stiffness degrades noticeably faster with increased levels of axial compression. Unfortunately, it is not clear how much of this difference can be attributed to the loading direction on material response versus that which may be attributed to the existence of residual stresses.
3. The stiffness reduction  $\tau$ -factor defined by equation 1 is conservative (but in the authors’ opinion not necessarily overly-conservative) in estimating the loss of axial stiffness due to increased levels of compressive force.

## 5 COMPUTATIONAL STUDY

Using one of the frames appearing in the original AISC calibration studies mentioned above, a computational study was performed to investigate the impact of adopting the AISC  $\tau$ - and 0.8 factors within the AA provisions. The symmetrical portal frame used in this study is shown in figure 2. Two ratios of beam-to-column stiffness were considered, one of which included assuming rigid beams with  $(EI/L)_c/(EI/L)_b = 0$ , and the other with moderately flexible beams  $(EI/L)_c/(EI/L)_b = 3$ . Using the cross-section geometry of the bi-symmetrical I-shape used in the above experimental study, both major- and minor-axis bending behavior of the columns was investigated. In all cases, members were assumed fully braced out-of-plane.

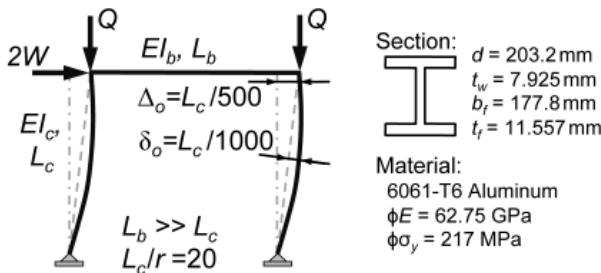


Figure 2: Symmetrical portal frame used in computational study.

For each of the four models investigated, two nonlinear finite element programs were employed to determine system strengths and obtain interaction curves for a wide range of resulting combinations of axial force and bending in the columns.

A more refined and commercially available finite element program ADINA [8] was employed to obtain a theoretically “exact” solution. Three-dimensional models of the I-shape were created using fully integrated, 4-node shell elements (MITC4). The cross section was modeled with a mesh density of 10 elements across the flange width and 10 elements through web depth. The number of elements along the

length of the member was varied to maintain an element aspect ratio of approximately one. A typical model included approximately 6000 shell elements. All models considered both geometric (large rotation/small strain) and material (multi-linear plasticity) nonlinear effects. A nonlinear stress-strain response (figure 4) for aluminum was explicitly incorporated. Initial imperfections, including member out-of-straightness and frame out-of-plumb, were included by distorting the original finite element mesh. Because the focus of the study was to determine the impact of partially yielded compressive members on system stability, beam elements were always modeled as elastic and column elements were permitted to yield by using the constitutive relationship shown in figure 3.

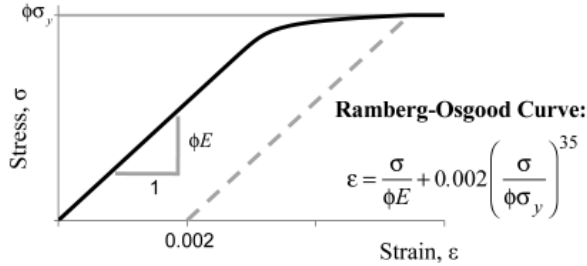


Figure 3: Stress-strain relationship used in ADINA analyses.

Each ADINA analysis was performed until a strength limit state was detected. Such limit states were typically defined by an instability resulting from a combination of yielding in the columns and second-order effects.

The frame analysis software MASTAN2 [9] was employed to obtain results that meet the above AA Specification’s stability requirements. MASTAN2 models second-order effects through the use of element geometric stiffness matrices and an incremental solution scheme based on an updated Lagrangian formulation [10]. Equation 1 is directly included in the analysis, which results in the flexural stiffness being reduced according to the axial force in each element during every load increment.

Strength limit states for the MASTAN2 analyses were defined by the combination of axial force and bending moment in the columns that just satisfied the AA Specification’s interaction equation:

$$\left| \frac{P_r}{P_c} + \frac{M_r}{M_c} \right| \leq 1.0 \tag{2}$$

where,  $P_r$  and  $M_r$  are the axial force and bending moment from the MASTAN2 analysis,  $P_c$  the design compressive strength determined in accordance with the AA Specification’s column curve with  $kL = L$ , and  $M_c$  the design strength determined in accordance with the AA Specification’s requirements for flexure (which for this fully braced compact section column,  $M_r = \phi_b S \sigma_y$  with  $\phi_b = 0.9$  and  $S$  is the elastic section modulus). Frame out-of-plumbness of  $H/500$  was included in these analyses but member out-of-straightness was not. The latter is assumed to be included in the AA Specification’s equation for column strength  $P_c$ .

## 6 RESULTS

Using the same validation approach employed in the AISC studies, the AA Specification stability requirements can be assessed by comparing  $P$ - $M$  interaction plots of the limiting strengths from the AA-MASTAN2 approach to the “exact” strength determined from sophisticated geometric and material nonlinear ADINA analyses.

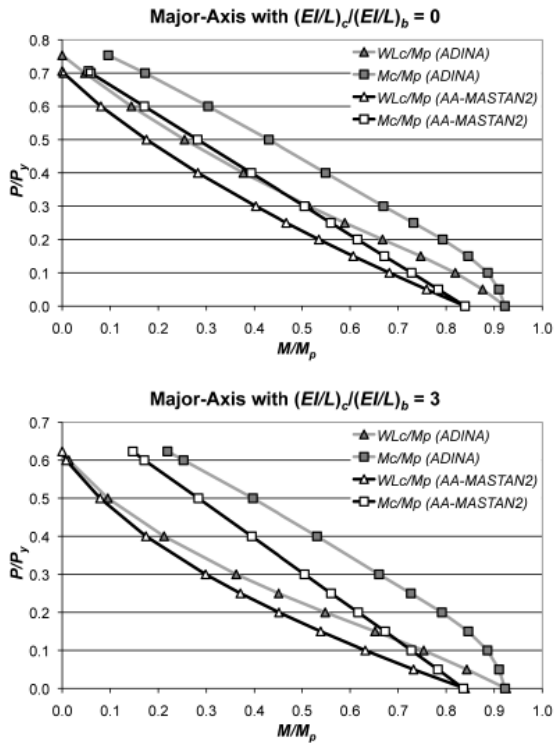


Figure 4: Interaction curves for major-axis bending of column.

Results for major-axis and minor-axis bending cases are contained in Figures 4 and 5, respectively. Two plots are presented in each figure, including one for rigid beams with  $(EI/L)_c/(EI/L)_b = 0$  and one for a moderate degree of flexibility in the beams with  $(EI/L)_c/(EI/L)_b = 3$ . Two sets of AA-MASTAN2 and ADINA curves are provided in each plot.

The first set allows for a comparison of the ratios of the first-order moment in the column to its plastic moment ( $WL_c/M_p$ , with  $W$  and  $L_c$  defined in figure 2, and  $M_p = Z\sigma_y$  where  $Z$  is the plastic section modulus). The second set can be used to compare ratios of the total moment (including first- and second-order effects) in the column to its plastic moment ( $M_c/M_p$ ). Each point on the curves represents the results of an analysis for specific combination of gravity load  $Q$  and lateral load  $W$ . In total, just under 50 separate ADINA and MASTAN2 analyses were performed in this study.

Based on Figures 4 and 5, several observations can be made:

1. For each analysis type (AA-MASTAN2 and ADINA), a comparison of the first-order moment ratio  $WL_c/M_p$  to the total moment ratio  $M_c/M_p$  at various values of  $P/P_y$  indicates that second-order effects are significant for this example. At loads as small as  $P/P_y = 0.1$ , the second-order moments are on the order of 10 to 15 percent larger than the first-order moments. As expected, this moment amplification increases significantly for larger values of  $P/P_y$ . The reason the ADINA second-order effects are larger is because this analysis includes material nonlinear behavior, which tends to reduce lateral stiffness and increase deflections.
2. By comparing the AA-MASTAN2 and ADINA total moment ratios  $M_c/M_p$  at various values of  $P/P_y$ , it is clear that the “exact” bending moment capacity of the column in the presence of any amount of axial force always exceeds the moment capacity defined by the AA Specification’s

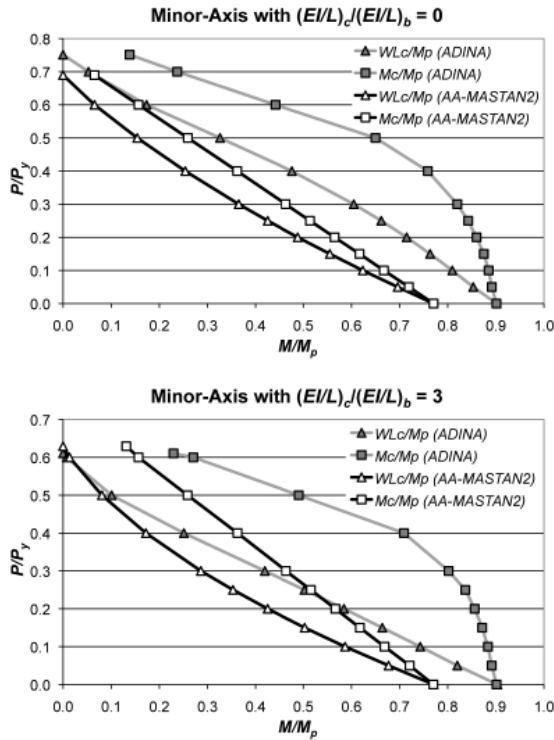


Figure 5: Interaction curves for minor-axis bending of column.

beam-column interaction equation (see equation 2). A significant factor contributing to this is that the AA Specification moment capacity of the member  $\phi_b \sigma_y Z$ , is less than the actual (ADINA) upper limit capacity of  $\phi_b \sigma_y Z$ . Another cause for this is that the AA Specification uses a single linear interaction equation to represent the strength of beam-columns; in most other specifications (e.g., AISC) a bilinear curve is used, which permits larger strengths at low- to intermediate values of axial force, ranging from approximately  $P/P_y = 0.1$  to  $P/P_y = 0.5$ .

3. The  $WL_c/M_p$  curves also provide a direct indication of the ultimate strength of the frame predicted by the AA-MASTAN2 and ADINA approaches. For example, the coordinate pair  $(WL_c/M_p, P/P_y) = (0.2, 0.4)$  represents failure at gravity and lateral load combination of  $Q = 0.4P_y$  and  $W = 0.2M_p/L_c$ . In all major-axis bending cases, the strength predicted by the AA-MASTAN2 approach is less than the “exact” strength predicted by ADINA. This conservatism is repeated for all minor-axis bending conditions with the exception of the high axial load case ( $P/P_y > 0.5$ ) in the frame with a moderately flexible beam of  $(EI/L)_c/(EI/L)_b = 3$ . The over-predicted AA-MASTAN2 strength, however, is quite small (see lower plot in figure 4). For a column-to-beam stiffness of  $(EI/L)_c/(EI/L)_b = 3$ , a design method based on effective length would use an effective length factor of approximately  $k = 2.5$ , whereas the AA stability provisions permit the use of  $k = 1.0$ .
4. The largest  $P/P_y$  values observed in each AA-MASTAN2 case are between 0.6 and 0.7. Substituting these values into equation 1 results in relatively inconsequential  $\tau$ -factors of 0.96 and 0.84, respectively. Given that fairly stocky columns ( $L/r = 20$  with  $r = \sqrt{I/A}$ ) were investigated in this study, it should be noted that larger slenderness  $L/r$  values more common to

design would result in smaller column strengths (i.e. lower  $P/P_y$  values) and hence, even larger (closer to 1.0) and less consequential  $\tau$ -factors.

## 7 SUMMARY/CONCLUSION

The new stability provisions that appear in the 2010 Aluminum Association's *Specification for Aluminum Structures* have been investigated by a study that contains experimental and analytical components. Experimental stub-column tests were performed on I- and hollow-rectangular shapes in an effort to better understand the reduction in axial stiffness in the presence of compressive force. Computational analyses were then performed on a portal frame that is similar to one used in part to validate the AISC stability provisions. In this work, various combinations of lateral and gravity loads were examined as well as varying degrees of frame flexibility.

Insight from this study indicates that use of the AA stability provisions in conjunction with the AA single linear interaction equation for designing beam-columns provides moderate to fairly conservative results. The AA use of the same stiffness reduction factors  $\tau$  and 0.8 that appear in the AISC Specification does not appear to be unreasonable, although it is unclear if the  $\tau$ -factor is necessary.

The study presents several cases where the AA stability provisions are adequate for allowing the routine use of an effective length factor of  $k = 1$ , even in cases where an effective length design method requires using two to three times that value. Just as importantly, the research further justifies the need to consider second-order effects in the design of aluminum structures.

It is recommended that additional studies be made to determine if the AA could avoid the use of a  $\tau$ -factor in future editions to their specification. Such studies should also explore cases that include built-up sections, where the effects of welding may result in substantial residual stresses and may justify using the  $\tau$ -factor.

## 8 ACKNOWLEDGEMENT

The authors thank the Aluminum Association for their support of this research under grant number 547.

## REFERENCES

- [1] Aluminum Association, *Specification for Aluminum Structures*, Arlington, VA, 2010.
- [2] American Institute of Steel Construction, *Specification for Structural Steel Buildings*, Chicago, IL, 2010.
- [3] Surovek-Maleck, A., White, D.W. and Ziemian, R.D., *Validation of the Direct Analysis Method*, Structural Engineering, Mechanics and Materials Report No. 35, School of Civil and Environmental Engineering, Georgia Institute of Technology, Atlanta, GA, 2003.
- [4] Bleich, F., *Buckling Strength of Metal Structures*, McGraw-Hill, New York, 1952.
- [5] Kissell, J.R. and Ferry, R.L., *Aluminum Structures: A Guide to Their Specifications and Design*, Wiley, Hoboken, NJ, 2002.
- [6] Ziemian, R.D. (Ed.), *Guide to Stability Design Criteria for Metal Structures*, 6<sup>th</sup> edition, Wiley, Hoboken, NJ, 2010.
- [7] ASTM Standard B557, *Standard Test Methods for Tension Testing Wrought and Cast Aluminum- and Magnesium-Alloy Products*, ASTM International, West Conshohocken, PA, 2006.
- [8] ADINA, Theory Manual, ADINA Research and Development, Inc., Watertown, MA, 2009.
- [9] MASTAN2, developed by R.D. Ziemian and W. McGuire, version 3.2, www.mastan2.com, 2009.
- [10] McGuire, W., Gallagher, R.H., and Ziemian, R.D., *Matrix Structural Analysis*, Wiley, Hoboken, NJ, 2000.